www.czasopisma.pan.pl PAN POLSKA AKADEMIA NAUK www.journals.pan.pl

Arch. Metall. Mater. **63** (2018), 1, 403-411

DOI: 10.24425/118954

W. MOĆKO*#, C. KOSTRZEWSKI*, A. BRODECKI*

INFLUENCE OF ANISOTROPY ON THE VISCOPLASTIC PROPERTIES OF A HOT ROLLED Ti6Al4V TITANIUM ALLOY

In this work, the influence of strain rate on the anisotropy of the Ti6Al4V titanium alloy has been analyzed. Tensile tests of notched specimens were carried out in three loading orientations (0°, 45°, and 90°) with respect to the rolling direction, using the servo-hydraulic testing machine and Hopkinson bar. Investigation was supported by the digital image correlation analysis of strain distribution on the specimen surface and assessment of the fracture mechanism. The Ti6Al4V titanium alloy reveals a typical strain rate hardening behavior; however, strain rate sensitivity is independent of the loading orientation. Increases of the loading orientation results in material softening, observed as lowered yield stress, whereas plastic strain exponent and modulus remain unaffected. Fracture strain decreases with loading orientation at quasi-static and dynamic loading conditions.

Keywords: Hopkinson bar, Digital image correlation, Titanium alloy, Constitutive relation, Anisotropy, High strain rate, Hill's potential

1. Introduction

1.1. Mechanical properties

Titanium alloys, including Ti6Al4V grade, reveal outstanding corrosion resistance, high strength, and low weight ratio. Therefore, they are often used in many demanding applications, which require high-performance materials, that is, in fields such as aerospace as well as medicine, automotive, power generation, sports, and chemical plants. The manufacturing process may introduce some texture into materials and therefore induce anisotropy of mechanical properties. Inducing this anisotropy in a fully controlled way may be a part of the structural designing process aimed at strengthening material properties in heavy loaded directions, and at the same time, reducing load capacity in other ones. The texture, induced in materials as a consequence of rolling, leads to the formation of specific crystallographic features and influences the activities of dislocation slips and twinning. The deformation mechanism depends on the loading direction, consequently leading to anisotropic deformation. Material yielding is dominated by dislocation slips, and the change of yielding mechanism with the loading direction (prismatic slip for the rolling direction – RD and transversal direction – TD, and basal slip for the normal direction – ND) resulted in yielding anisotropy [1]. It was found that for the Ti6Al4V titanium alloy treated by unidirectional hot rolling, yield strength and tensile strength ratio determined between specimens cut in rolling (RD) and transversal (TD) directions depend on the rolling temperature. The ratio estimated for a processing temperature equal to 830°C was equal to 1, whereas increase of rolling temperature to 920°C increased ratio to 1.1. It was also shown that the application of the cross-rolling method enables to diminish anisotropy of mechanical properties [2]. Other investigations carried out for hot rolled Ti6Al4V titanium alloy sheet show that cold rolling of as-received material also influences the stress-strain behavior. The highest flow stress was estimated at orientation $\theta = 90°$, whereas the lowest stress was determined at orientation $\theta = 45°$ for the material initially cold rolled in four various directions with respect to the hot rolling direction during fabrication. Moreover, strain at fracture was also orientation dependent, that is, the lowest strain was obtained for $\theta = 90°$ and highest for $\theta = 45°$ [3]. Quasi-static tension and compression test of the Ti6Al4V titanium alloy carried out at room temperature for specimens cut at three orthogonal directions (longitudinal, transversal, and thru thickness) show that the material reveals both yield stress anisotropy and tension/compression asymmetry. Furthermore, the anisotropy under compression is more pronounced than under tension [4]. Plastic anisotropy and associated deformation mechanisms of rolling textured, high-purity, alpha-phase titanium were investigated by carrying out uniaxial compression tests along the three featured directions – the rolling direction (RD), normal direction (ND), and transverse direction (TD) – in combination with an electron backscatter diffraction measurement and a Schmid factor (SF) analysis. The results revealed that the specific crystallographic feature of the material caused by the rolling texture influences the activities

* MOTOR TRANSPORT INSTITUTE, 80 JAGIELLOŃSKA STR., 03-301 WARSAW, POLAND

Corresponding author: wojciech.mocko@its.waw.pl

of dislocation slips and twinning by affecting their SF, and this significantly varies with the loading direction, consequently leading to anisotropic deformation. The high strain-rate tension tests performed using the split Hopkinson tension bar apparatus indicates that the tension responses of the Ti6Al4V titanium alloy are dependent on the temperature and strain rate. The values of the initial yield stress decrease with increasing temperature and increase significantly with increasing strain rate. However, the isothermal strain-hardening behavior is essentially independent of the strain rate and temperature [5]. Static and dynamic shear, uniaxial tensile, and plain strain tests on Ti6Al4V sheet show that the strain rate has an important effect only on the fracture strain in shear [6].

1.2. Constitutive modelling and anisotropic yield criterion

Finite element code requires a good fitted constitutive equation in order to predict the mechanical behavior of structure with good accuracy. In the case of anisotropic materials, this model consists of two parts, that is, flow stress definition including influence of strain, strain rate, and temperature on the overall stress and yield locus description, taking into account material anisotropy. The form of constitutive relation depends on the crystalline structure of a given material. The Ti6Al4V titanium alloy contains two phases, that is, $\alpha+\beta$. Since the content of BCC structure β phase is low, the influence of the slip in this phase on the overall plastic deformation of the alloy is very limited. The majority of the plastic strain is accommodated by the HCP α phase, and texture evolution is not noticeably affected by slip in the β phase; thus, the deformation behavior is dominated by the α phase with limited slip systems [7]. Taking into account the low content of β phase, it may be assumed that plastic properties of the Ti6Al4V alloy depend mainly on the α phase with HCP crystalline microstructure. Among many constitutive models applicable for the purposes of HCP modeling, two major types may by distinguished. The first group including Johnson-Cook (JC) [8], Norton-Hoff (NH) [9], and Khan-Huang-Liang (KHL) [10] and Litonski [11] takes into account the phenomenological basis. The latter type of relation, that is, the mechanical threshold strength (MTS) [12], Zerilli-Armstrong (ZA)) [13], and Nemat-Nasser (NN) [14], is physically based. Rusinek and Klepaczko (RK) also proposed a universal constitutive model in which equivalent stress is decomposed into internal stress and effective stress. The developed relation was successfully applied to predict mechanical properties of metals with FCC structure [15,16] as well as BCC structure [15]. Application of this equation was extended for prediction of the Ti6Al4V titanium alloy characterized by HCP crystalline structure [17].

The first anisotropic model introduced by Hill was based on the von-Mises yield criterion [18]. This work was extended in the following years by the next researcher [19-22], however with certain assumptions that compressive and tensile yield are of equal value. Since for hexagonal closed packed metals (HCP) including Ti6Al4V titanium alloy, asymmetry between tension and compression must be taken into account, for this type of crystalline structure, improved yield criteria were proposed [23]. This model takes into account both anisotropy of a material and yielding asymmetry between tension and compression. The anisotropic yield stress may be determined on the basis of proposition of an energy-based hypothesis of material effort for anisotropic materials exhibiting strength differential effect introduced by Ostrowsk-Maciejewska et al. [24].

1.3. Scope of work

In this work, tensile tests of the Ti6Al4V titanium sheet at three planar orientations were carried out. Tensile tests were done at quasi-static and dynamic deformation regime in order to examine the influence of strain rate on the anisotropy of the material. Since compression tests were omitted, the basic Hill's criterion implemented into ABAQUS software was used to predict yield locus and obtain a good agreement with experimental data. The presented analysis is an extension of previous works where the RK model was applied to determine the mechanical response of the Ti6Al4V titanium alloy in single RD orientation [25]. Here, the RK constitutive relation, together with Hill's criterion, was used to estimate tensile titanium alloy properties at a wide range of strain rates and loading orientations. Up to this moment influence of the strain rate on the anisotropy of yield strength was not fully analysed. In this paper a number of experiments and investigations were carried out to correlate viscoplastic properties with loading direction and strain rate.

2. Experimental characterization

2.1. Material and specimen

Material was delivered in a form of hot rolled Ti6Al4V titanium alloy sheet of 3 mm thickness. The chemical composition of the material is presented in Table 1. The specimens were cut along three orientations with respect to the rolling direction, that is, RD – along, 45D – 45 degree and TD – transverse to rolling direction, as shown in Fig. 1. Notched specimens with gauge length equal to 10 mm were applied to enable a high strain rate testing using the tensile Hopkinson bar. The same geometry was applied for both quasi-static and dynamic testing. Specimen geometry and dimensions are presented in Fig. 2. Specimens were cut using electro-discharge machining (EDM).

TABLE 1

Chemical composition of Ti6Al4V according to quality certificate delivered by supplier [%]

Ti	Al	V	Fe	C	N	O	H
Balance	6.0	4.0	≤0.40	≤0.08	≤0.05	≤0.20	≤0.015

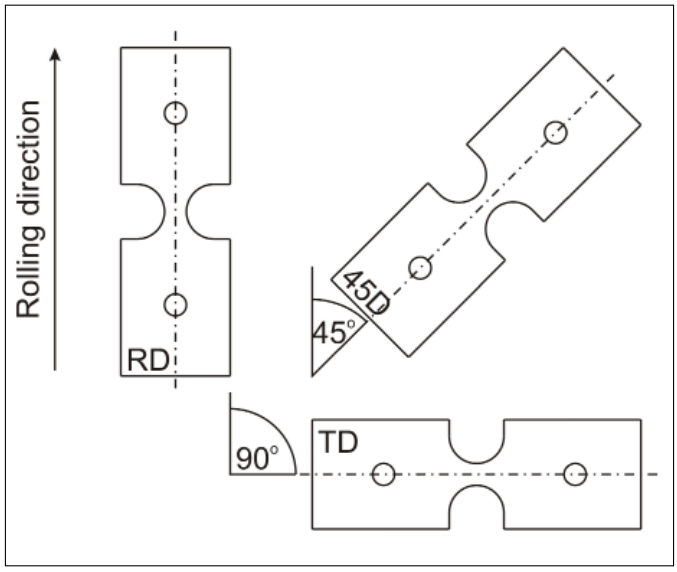

Fig. 1. Scheme of specimen orientation with respect to the sheet rolling direction

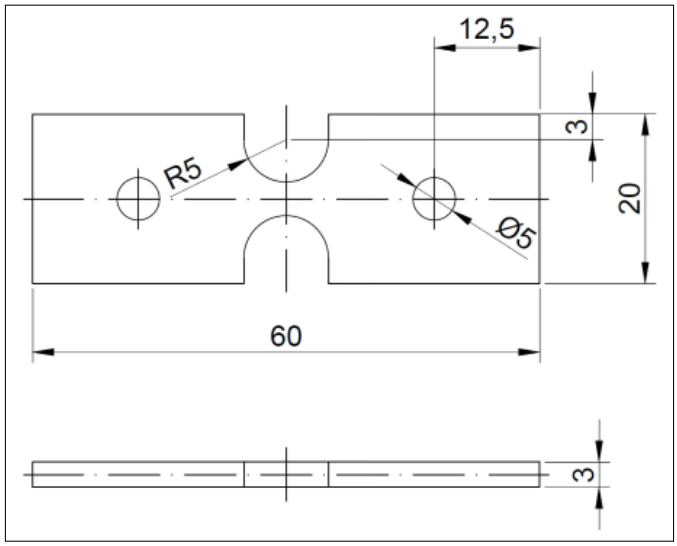

Fig. 2. Specimen geometry (dimensions in mm)

2.2. Tensile tests

Tensile tests were carried out at quasi-static and dynamic loading regime using, respectively, Instron servo-hydraulic testing machine and pre-tension split Hopkinson bar [26,27]. The testing stand at the Motor Transport Institute comes with bars 20 mm in diameter made of 7075-T6 aluminum alloy [17,28,29]. The incident bar, which is 3600 mm long, is divided into a pre-tension section with a length of 1600 mm and a free end.

2.3. Digital image correlation method

For determining strain components at quasi-static deformation rates, the ARAMIS 4M video system with resolution equal to 2400 × 1728 pixels was used [17,28]. The videos recorded during the experiments were then analyzed by the digital image correlation (DIC) method implemented in the ARAMIS software to determine 2D field of displacement. At dynamic loading conditions, the test was recorded using Phantom V1210 fast camera at a resolution of 384 × 128 and a frame rate equal to 150,000. Video recorded using a high-speed camera was subsequently analyzed using the ARAMIS software.

2.4. Anisotropic yield criterion

Elastic range was assumed to be isotropic, whereas the influence of loading direction on the plastic behavior of metal sheet may be presented with the use of a quantity called Lankford parameter or anisotropy coefficient [30]. Usually this coefficient is determined by uniaxial tensile tests on sheet specimens in the form of a strip. However, in this work, short-notched specimens with strain localization were applied in order to enable a high strain rate Hopkinson bar test. To determine strain components along rolling, transverse, and normal directions, the DIC technique was applied. Assuming strain components notation ε_{11}, ε_{22}, and ε_{33}, respectively, in loading, transverse, and normal directions, the anisotropy coefficient r may be defined by:

$$r = \frac{\varepsilon_{22}}{\varepsilon_{33}} \tag{1}$$

For the isotropic materials, the coefficient is equal to 1. Since DIC analysis software actually determines plastic deformation of the specimen in a thru-thickness direction ε_{33} on the basis of planar strain components ε_{11}, ε_{22}, assuming volume constancy conditions expressed as follows:

$$\varepsilon_{11} + \varepsilon_{22} + \varepsilon_{3}3 = 0 \tag{2}$$

therefore, anisotropy coefficient may be expressed using planar strain components as:

$$r = \frac{-\varepsilon_{22}}{\varepsilon_{11} + \varepsilon_{22}} \tag{3}$$

The anisotropic yielding was modeled using the Hill's criterion expressed in terms of rectangular Cartesian stress components as:

$$f(\sigma) = \sqrt{\begin{aligned} &F(\sigma_{22} - \sigma_{33})^2 + G(\sigma_{33} - \sigma_{11})^2 + \\ &+ H(\sigma_{11} - \sigma_{22})^2 + 2L\sigma_{23}^2 + 2M\sigma_{31}^2 + 2N\sigma_{12}^2 \end{aligned}} \tag{4}$$

where F, G, H, L, M, and N are constants obtained by tests of the material in different orientations. They are defined as:

$$F = \frac{(\sigma^0)}{2}\left(\frac{1}{\bar{\sigma}_{22}^2} + \frac{1}{\bar{\sigma}_{33}^2} - \frac{1}{\bar{\sigma}_{11}^2}\right) = \frac{1}{2}\left(\frac{1}{R_{22}^2} + \frac{1}{R_{33}^2} - \frac{1}{R_{11}^2}\right) \tag{5}$$

$$G = \frac{(\sigma^0)}{2}\left(\frac{1}{\bar{\sigma}_{33}^2} + \frac{1}{\bar{\sigma}_{11}^2} - \frac{1}{\bar{\sigma}_{22}^2}\right) = \frac{1}{2}\left(\frac{1}{R_{33}^2} + \frac{1}{R_{11}^2} - \frac{1}{R_{22}^2}\right) \tag{6}$$

$$H = \frac{(\sigma^0)}{2}\left(\frac{1}{\bar{\sigma}_{11}^2} + \frac{1}{\bar{\sigma}_{22}^2} - \frac{1}{\bar{\sigma}_{33}^2}\right) = \frac{1}{2}\left(\frac{1}{R_{11}^2} + \frac{1}{R_{22}^2} - \frac{1}{R_{33}^2}\right) \tag{7}$$

$$L = \frac{3}{2}\left(\frac{\tau^0}{\bar{\sigma}_{23}}\right)^2 = \frac{3}{2R_{23}^2} \tag{8}$$

$$M = \frac{3}{2}\left(\frac{\tau^0}{\bar{\sigma}_{13}}\right)^2 = \frac{3}{2R_{13}^2} \tag{9}$$

$$N = \frac{3}{2}\left(\frac{\tau^0}{\bar{\sigma}_{12}}\right)^2 = \frac{3}{2R_{12}^2} \tag{10}$$

where each $\bar{\sigma}_{ij}$ is the measure yield stress value when σ_{ij} is applied as the only nonzero stress component; σ^0 is reference stress specified for the metal plasticity definition $R_{11} = \bar{\sigma}_{11}/\sigma^0$, $R_{22} = \bar{\sigma}_{22}/\sigma^0$, $R_{33} = \bar{\sigma}_{33}/\sigma^0$, $R_{12} = \bar{\sigma}_{12}/\tau^0$, $R_{13} = \bar{\sigma}_{13}/\tau^0$ and $R_{23} = \bar{\sigma}_{23}/\tau^0$, are anisotropic yield stress ratios; and $\tau^0 = \sigma^0/\sqrt{3}$.

2.5. Metal plasticity definition

Metal plasticity was defined with the use of the Rusinek Klepaczko evolution equation of flow stress. Application of this model to predict mechanical response of Ti6Al4V titanium alloy under uniaxial tensile test was already introduced in a previous work [25].

The overall flow stress in the Rusinek-Klepaczko model [31] was decomposed into three stress components: the internal stress $\bar{\sigma}_\mu(\bar{\varepsilon}^p, \dot{\bar{\varepsilon}}^p, T)$, the effective stress $\bar{\sigma}^*(\dot{\bar{\varepsilon}}^p, T)$, and the drag stress $\bar{\sigma}_d(\dot{\bar{\varepsilon}}^p)$ as shown in Eq. 11.

$$\bar{\sigma}\left(\bar{\varepsilon}^p, \dot{\bar{\varepsilon}}^p, T\right) = \frac{E(T)}{E_0}\left[\begin{matrix}\bar{\sigma}_\mu\left(\bar{\varepsilon}^p, \dot{\bar{\varepsilon}}^p, T\right) + \\ +\bar{\sigma}^*\left(\dot{\bar{\varepsilon}}^p, T\right)\end{matrix}\right] + \bar{\sigma}_d\left(\dot{\bar{\varepsilon}}^p\right) \tag{11}$$

More details concerning application of the Rusinek-Klepaczko constitutive equation may be found in other papers [15,31-36].

3. Experimental results

3.1. Influence of specimen orientation on stress-strain curves

At the first stage of the experimental work force-displacement curves at quasi-static and dynamic loading conditions were determined. The characteristics were estimated using force and displacement transducer and elastic wave propagation theory, respectively, at servo-hydraulic testing machine and tensile Hopkinson bar. Each of the charts includes data acquired at three various strain rates, namely, $10^{-4}s^{-1}$, $10^{-2}s^{-1}$, and $6 \times 10^2 s^{-1}$. Subsequently, force-displacement characteristics were re-calculated as true stress-true strain curves using the DIC method. In order to obtain the true strain value, the axial strain component is determined using the optical field method. Further, true stress is calculated on the basis of true strain and force value. More details on this transformation may be found in the author's earlier work [25].

True stress-true strain characteristics of the Ti6Al4V titanium alloy determined at three loading orientations, that is, RD, 45D, and TD are shown in Fig. 3. It may be seen that independent of the material orientation, Ti6Al4V titanium alloy reveals both work and strain rate hardening. The results were compared with selected results of other researchers concerning analysis of mechanical properties of the Ti6Al4V titanium alloy. Results obtained by Khan in his work gives flow stress value lower than in this work. The difference equal to 200 MPa

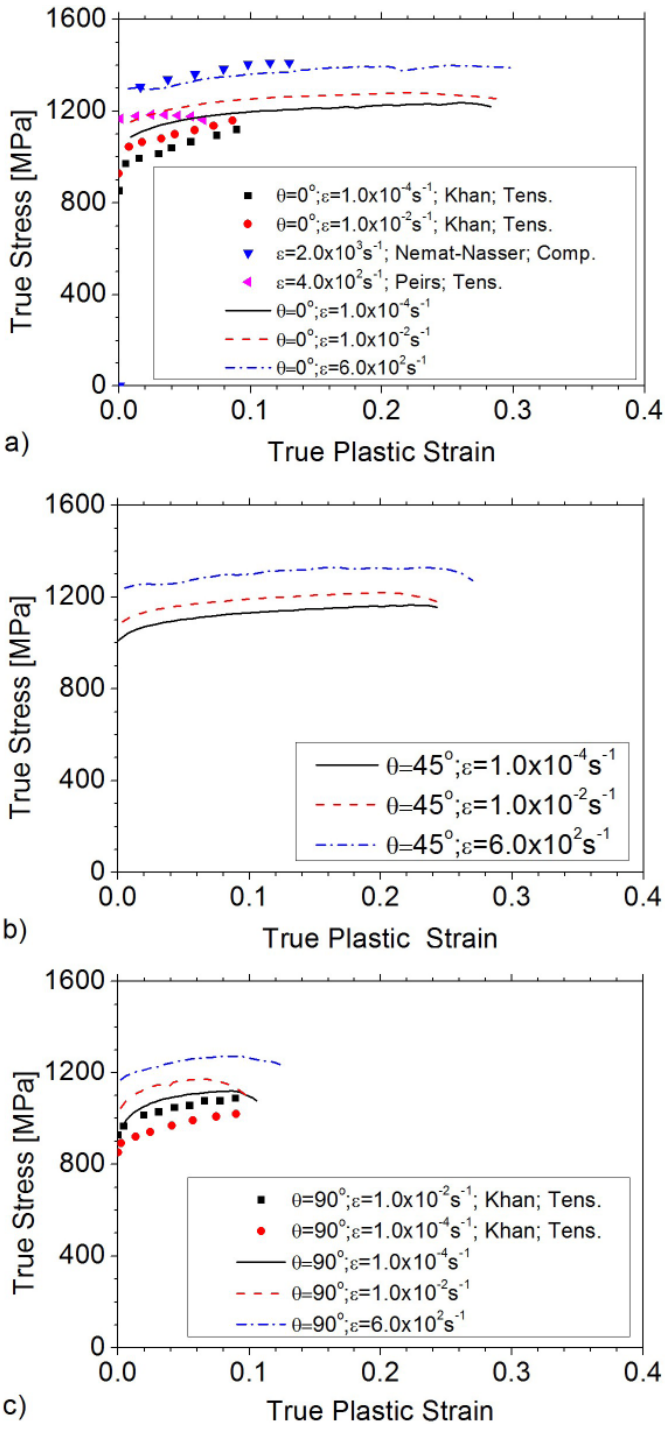

Fig. 3. Experimental true stress-strain curves for a specimen subjected to uniaxial tension (a) along rolling (RD), (b) 45° to the RD (45D), and (c) transverse (TD) directions at various strain rates compared with reference data [6,14,37]

is related to methodology of alloy processing applied by Khan, i.e. electron beam single melt Ti6Al4V alloy [37], whereas in this work hot rolled sheet was used. Despite other method of material manufacturing three similar phenomenon are observed for reference data [37] and the experimental data: strain rate hardening, work hardening and drop of the flow stress with the increase of loading direction. Data obtained during dynamic tensile tests specimens, cut by EDM from titanium alloy sheet of 0.6 mm thickness, provided by Peirs [6], are lower than experimental results determined using split Hopkinson tensile bar within scope of this work of about 100 MPa. But it should be noted that specimen loading orientation with respect to the rolling direction and material processing method were not clearly marked. Results obtained by Nemat-Nasser at dynamic compression for Ti6Al4V alloy test [14] shows good agreement with experimental data determined in this work. In-depth analysis carried out by Chichili shows that plastic deformation of titanium alloy induces an increase in the twin number density. At low strain rates, the twin number is significantly lower than the twin number estimated at high strain rates [36]. Independent of the plastic deformation mechanism (slip or twinning) strain hardening of analyzed alloy is essentially independent of strain rate and temperature [5]. Further analysis of the offset yield stress determined at a strain equal to 0.005 indicates that increase of loading orientation induces decrease of the yield stress (Fig. 4). Further analysis of the offset yield stress determined at a strain equal to 0.005 indicates that increase of loading orientation induces decrease of the yield stress (Fig. 4). Similar effect of loading orientation on the yield stress, i.e. lowering of the yield stress with the increasing loading angle were obtained by Won at quasi-static loading conditions. The yielding mechanism of HCP metals is governed by dislocation slips. A change of the yielding mechanism with the loading direction (prismatic <a> slip for the RD and TD, and basal <a> slip for the ND) gives drop to yielding anisotropy [1]. The same hardening effect is observed at all applied strain rates. Estimated difference of the yield stress between ND and TD is equal to about 100 MPa.

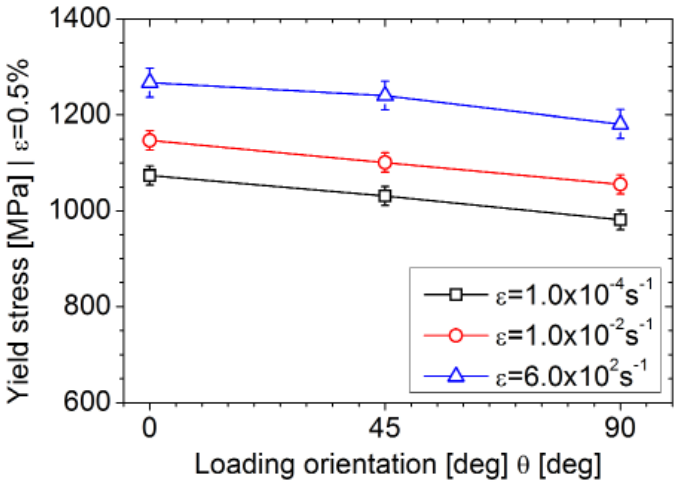

Fig. 4. Experimental tensile yield stress (0.5%) offset for three in-plane orientations θ measured with respect to the rolling direction

The influence of the specimen orientation on the strain rate sensitivity of Ti6Al4V is shown in Fig. 5. It may be observed that the value of inclination of the characteristic is comparable for all three loading directions, that is, RD, 45D, and TD. The average rate sensitivity defined as $\delta\sigma/\delta\dot{\varepsilon}$ is equal to 30 MPa/s^{-1}. Moreover, it may be observed that at an applied strain rate range, that is, from 10^{-4}s^{-1} to 6×10^{2}s^{-1} an increase of the flow stress is linearly dependent on the logarithm of the strain rate. A similar behavior of Ti6Al4V alloy determined for single-loading orientation at compressive and tensile loadings was also found by other researchers [6,14,36].

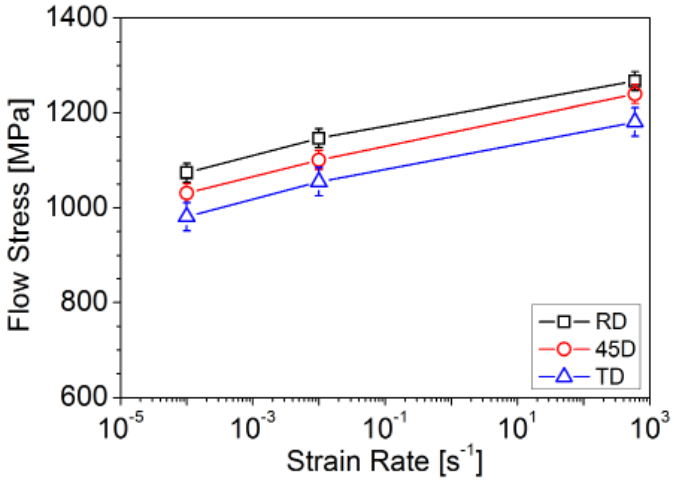

Fig. 5. Strain-rate sensitivity at various loading orientations determined at strain equal to 0.5%

The impact of the loading orientation on the fracture strain is shown in Fig. 6. At quasi static loading regime, fracture strain decreases from 0.29 through 0.24 down to 0.10, respectively, at orientation RD, 45D, and TD. It should be noted that results determined at both quasi-static strain rates, that is, 10^{-4}s^{-1} and 10^{-2}s^{-1}, are very close. The fracture behavior of the Ti6Al4V titanium alloy loaded using Hopkinson bar is similar to those determined at quasi-static conditions. After the minor decrease of fracture strain from 0.30 to 0.27 with the increase of orientation angle from 0° to 45°, a major increase of fracture strain to a value of 0.12 at loading angle equal to 90° was found. To summarize, the fracture strain within the full range of applied strain rates is the lowest (from 0.10 to 0.12) for specimens loaded along TD, whereas fracture strain values at other two orientations, that is, RD and 45D, are in range from 0.22 to 0.30. Fracture strain analysis of Ti6Al4V titanium alloy conducted under tensile loading conditions at a wide range of strain rates and loading orientation were not reported in the literature. The results available in the references show that fracture strain of the Ti6Al4V alloy may be rate dependent, that is, at quasi-static conditions the fracture strain was equal to 0.18, whereas at dynamic loading regime it dropped to 0.15 [38]. A similar behavior, that is, drop of fracture strain from 0.10 to 0.08, respectively, under quasi-static and dynamic loading conditions, was observed by Wang [5].

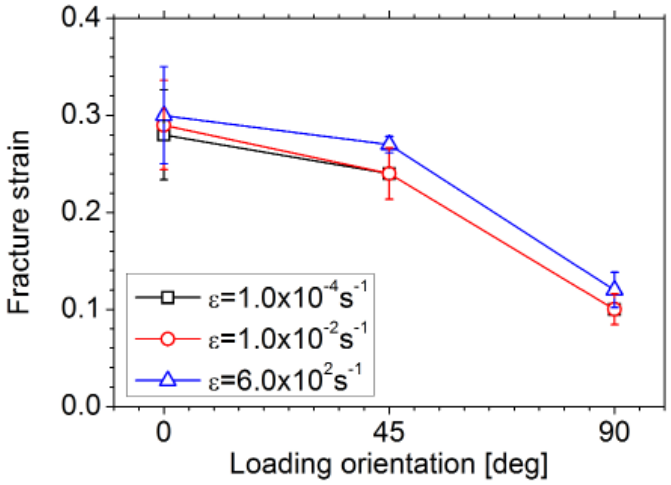

Fig. 6. Experimental strain at failure for three in-plane orientations θ measured with respect to the rolling direction

3.2. Lankford coefficients

The value of the Lankford coefficients defined as the ratio between the width and thickness (Eq. 1) are shown in Table 2. Presented data were determined using the linear interpolation function on the basis of curves shown in Fig. 7. It may be observed that Lankford coefficient estimated for loading direction equal to 90° is significantly lower than the same coefficients determined at two other orientations. The same relation is maintained at quasi-static and dynamic loading conditions as well. Small differences at particular loading orientation between low and high strain rate loading may be related to quite a large standard deviation of results rather than material properties.

TABLE 2

Average Lankford coefficients determined on the basis of data presented in Fig. 7 at various loading angles and strain rates

Deformation rate	Loading angle, [°]		
	0	45	90
Quasi-static	1.15	1.14	0.79
Dynamic	1.22	1.35	0.68

3.3. Optical field measurement of strain components distribution

The axial strain distribution determined under quasi-static and dynamic loading conditions for three loading orientations are shown in Fig. 8. Presented maps were acquired at the last frame before macroscopic material fracture. Strain distribution estimated for material loaded at TD is characterized by a wide area of strain of value equal to 0.1. Strain magnitude has almost constant value at almost the whole deformed area. Edges of plastically deformed zone are perpendicular to the loading force direction. The strain pattern determined for the specimen

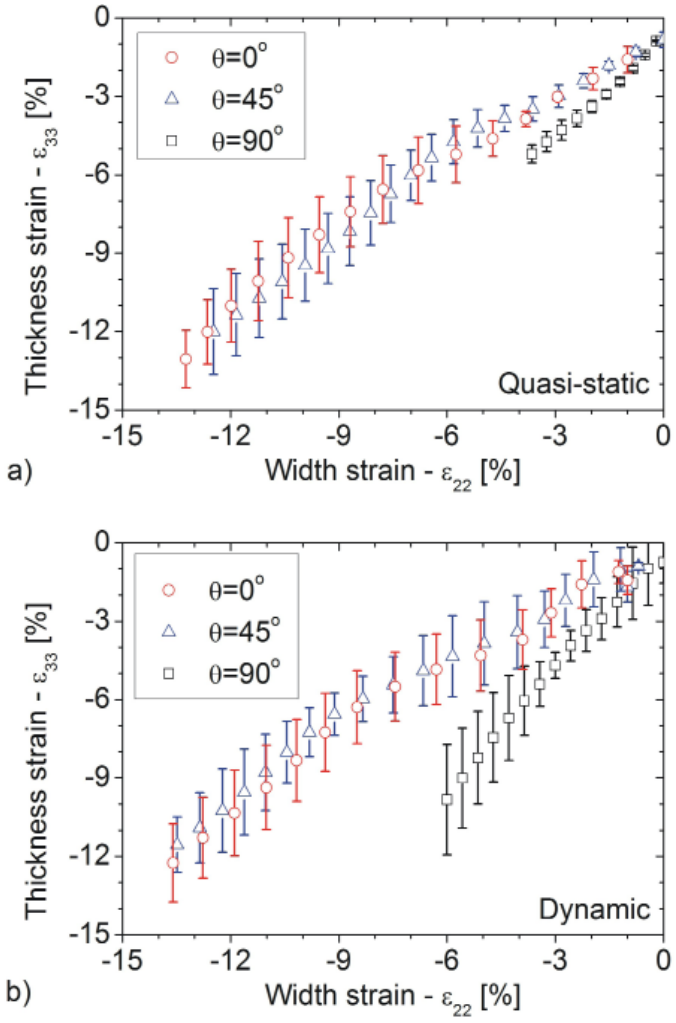

Fig. 7. Thickness strain vs. width strain for specimens cut at various directions with respect to the rolling directions determined using the DIC method at (a) quasi-static and (b) dynamic loading conditions

cut in 45D shows maximum strain line placed at 45° direction to the loading force. The value of maximum strain is close to 0.3. Ends of the plastically deformed zone, including area pre-strained up to 0.1, are perpendicular to the loading force. It may be observed that only the area of strain higher than 0.2 is oblique with respect to the loading direction. Analyzing axial strain distribution of the specimen cut in RD, it may be found that the plastic deformation zone is narrower than that for TD. Borders of pre-strained area are perpendicular to the loading direction, similarly to previous cases. Strain distribution along specimen axis incorporates clearly an observed maximum equal to 0.25 near the notch region. Different strain patterns depending on the loading angle, observed in Fig. 8, are result of the material anisotropy. Anisotropy of mechanical parameters, including fracture strain, yield stress and flow stress is illustrated in Fig. 3. Micromechanical origin of observed anisotropy in terms of plastic deformation mechanism will be matter of the future study. Comparison of axial strain distribution between quasi-static and dynamic loading conditions shows that plastic deformation pattern is very similar; however, maximum local strain values are higher at high strain rate tests.

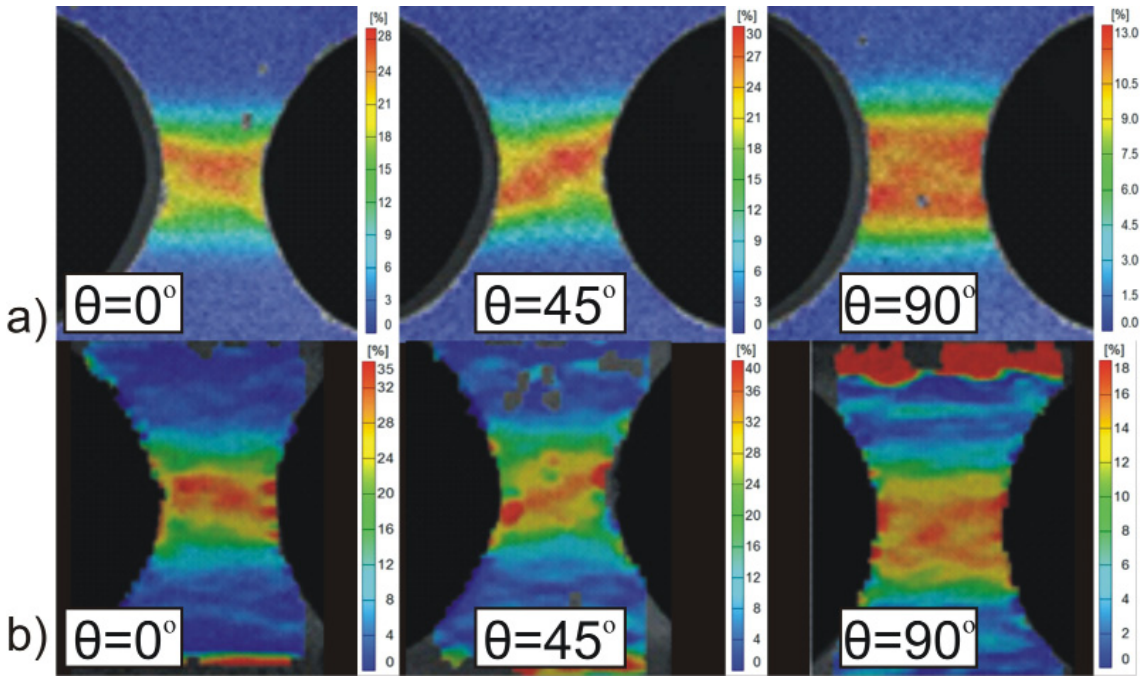

Fig. 8. Axial strain (ε_{11}) distribution determined using the DIC method at (a) quasi-static and (b) dynamic loading conditions for a specimen subjected to uniaxial tension along rolling (RD), 45° to the RD (45D), and transverse (TD) directions

3.4. Analysis of the fracture surface

The loading angle with respect to the rolling direction significantly affects strain distribution determined on the specimen surface. The effect of material texture is also clearly visible on the fracture surfaces obtained at various cut orientations. The typical surface of ductile material exposed to tensile loadings consists of a central part in which macroscopic fracture appears as a consequence of micro void generation and coalescence until crack formation and surrounding shear fracture zone. Analyzing the fracture surface of Ti6Al4V titanium alloy loaded at the transverse direction (Fig. 9a), it may be found that the crack area is divided into three rectangular zones of different inclinations. However, at each sub-surface, the material was broken as a result of shearing. Other two loading orientations, that is, 45D and RD reveal a typical ductile fracture mode with micro-void formation inside and shear zone outside. The shape of the internal micro-void formation zone has a shape similar to that of a rectangle for orientation 45D, whereas for orientation RD, the internal zone is of an elliptical shape.

4. Constitutive modeling

Obtained experimentally stress-strain curves were applied to calibrate RK constitutive relation and coefficients of Hill's potential. The calibration procedure of the RK model has been presented in detail in previous studies [27,28,31]. Coefficients of RK model and physical parameters are shown in Table 3 and Table 4, respectively. Physical basis of the particular coefficients of RK equation, listed in tables, were explained in previous works [23,29]. Hill's potential parameter R_{11} was assumed as equal to 1. Subsequently, R_{12} and R_{22} parameters were chosen using the interpolation function to give the best fit of stress-strain curves at various strain rates and both types of orientations, that is, R45 and TD. Obtained values are equal to 0.98 and 0.94 for coefficients R_{12} and R_{22}, respectively. A comparison of measured and calculated Ti6Al4V titanium alloy characteristics is shown in Fig. 10. Fig. 10 (a) presents results of tensile tests carried out in a wide range of strain rates at loading orientation with respect to the rolling direction equal to $\theta = 0°$. Coefficients of the RK model were calibrated at this orientation, assuming $R_{11} = 1$. It

TABLE 3

RK constitutive model parameters determined for the Ti6Al4V titanium alloy determined on the basis of experimental data

B_o (MPa)	v (–)	n_o (–)	D_2 (–)	ε_0 (–)	σ_0^* (MPa)	m^* (–)	D_1 (–)	χ (MPa)	α (s^{-1})	$\dot{\varepsilon}_{min}$ (s^{-1})	$\dot{\varepsilon}_{max}$ (s^{-1})
1230	−0.01	0.04	−0.01	0.01	210	0.2	0.58	100	1×10^{-5}	10^{-5}	10^{7}

TABLE 4

Physical parameters of the Ti6Al4V titanium alloy

E_0 (GPa)	θ^* (–)	C_p ($Jkg^{-1}K^{-1}$)	β (–)	ρ (kgm^{-3})	T_m (K)
115	0.9	470	0.9	4300	1570

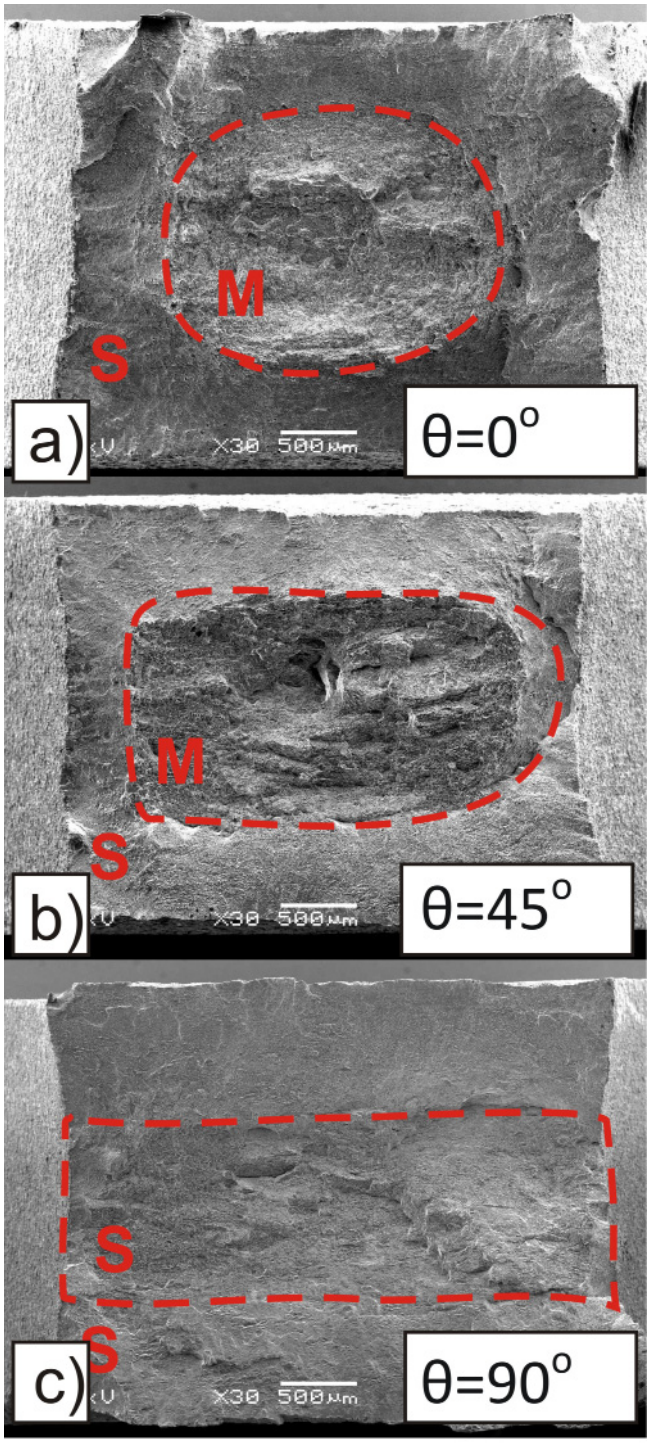

Fig. 9. Comparison of fracture surface obtained for three in-plane orientations θ measured with respect to the rolling direction at quasi-static loading conditions; S – shear fracture zone; M – micro void coalescence zone

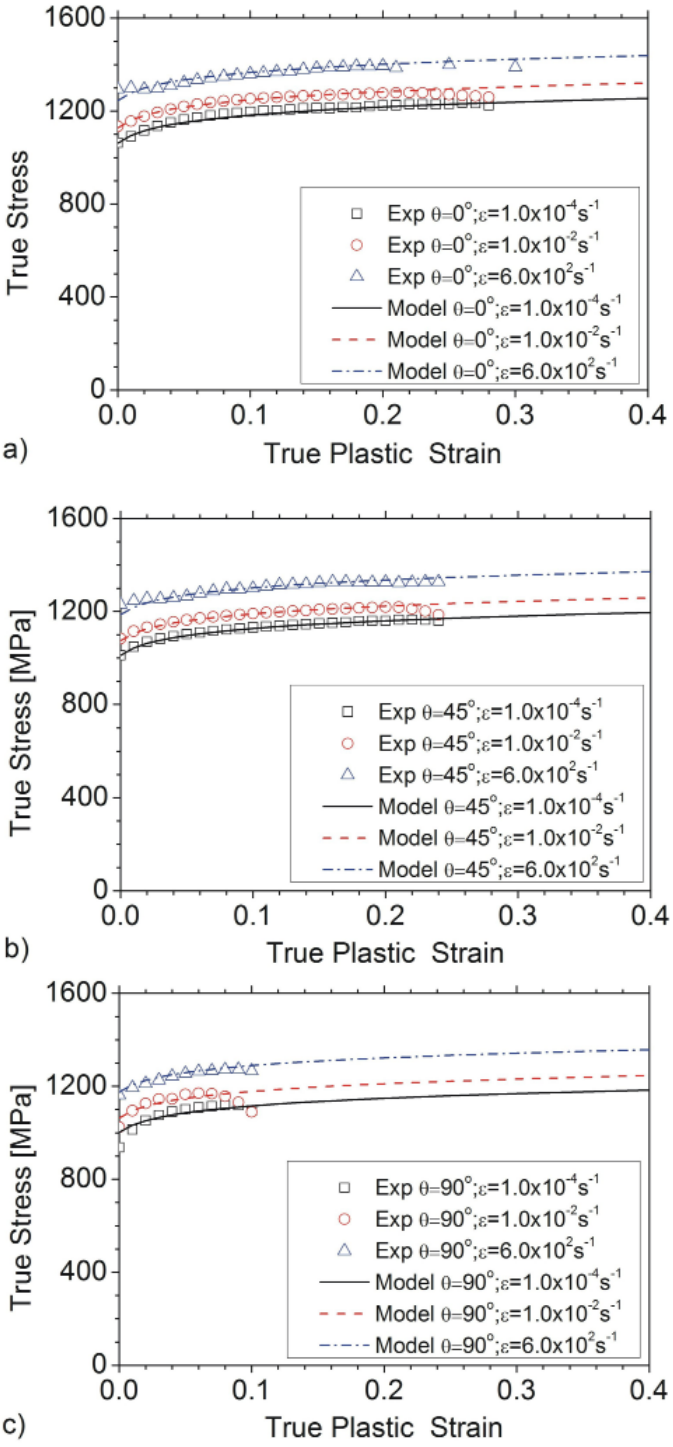

Fig. 10. Comparison of experimental and model-based true stress-strain curves for a specimen subjected to uniaxial tension (a) along rolling (RD), (b) 45° to the RD (45D) and (c) transverse (TD) direction at various strain rates

may be seen that yield stress, hardening modulus, and hardening exponent are in good agreement with experimental data.

5. Conclusions

On the basis of analysis of tensile tests of the Ti6Al4V titanium alloy carried out at three loading orientations with respect to the rolling direction and three various strain states from $10^{-4}s^{-1}$ to $6 \times 10^{2}s^{-1}$, the following conclusions may be drawn:

– The fracture strain decreases with loading orientation at quasi-static and dynamic loading conditions. At the loading orientation transversal to RD fracture strain is in the range from 0.10 to 0.12, whereas at loading orientation along RD fracture strain rises to a range from 0.28 to 0.30. Increase of strain rate induces increase of the fracture strain.

- Fracture surface of specimens loaded at orientation 45D and RD shows typical "cup and cone" behaviour with central micro-void formation zone and surrounding shear zone, whereas specimen loaded at RD shows three various shear zones.
- The Lankford's coefficient value is significantly lower at orientation $\theta = 90°$ than the orientation at another two values, that is, $\theta = 0°$ and $\theta = 45°$ at full range of analyzed strain rates.
- Axial and width strain strongly depend on the loading orientation: at RD, strain distribution includes clearly to observe maximum located transversally to the loading force; at 45D, it results in a strain distribution with clearly to observe maximum oblique to the loading direction; and finally at TD, it gives a wide area of uniform strain values close to 0.1 and positioned transversal to the loading direction. Under dynamic loading conditions determined locally, axial strain maximum values are higher than corresponding values estimated at quasi-static loading conditions. The width strain is insensitive to strain rates.
- The application of the RK constitutive equation together with Hill's criterion to predict anisotropic properties of Ti6Al4V titanium alloys sheet results in a good agreement with experimental and numerical results.

Acknowledgements

This study was supported by the Polish National Centre for Research and Development (GRAF-TECH/NCBR/14/26/2013)

REFERENCES

[1] J.W. Won, C.H. Park, S.-G. Hong, C.S. Lee, J. Alloy Compd. **651**, 245-254 (2015).
[2] Song J.-H., Hong K.-J., T.K. Ha, Mat. Sci. Eng. A **449-451**, 144-148 (2007).
[3] H. Francillette, M. Benmaouche, N. Gauquelin, J. Mater. Process. Tech. **198**, 86-92 (2008).
[4] V. Tuninetti, G. Gilles, O. Milis, T. Pardoen , A.M. Habraken, Int. J. Plast. **67**, 53-68 (2015).
[5] J. Zhang, Y. Wang, Mat. Sci. Eng. A **605**, 59-64 (2014).
[6] J. Peirs, P. Verleysen, J. Degrieck, Procedia Engineering **10**, 2336-2341 (2011)
[7] L.-Q. Yang, Y.-Q. Yang, Deformed microstructure and texture of Ti6Al4V alloy. Trans. Nonferrous Met. Soc. China 24, 3103-3110 (2014).
[8] G.R. Johnson, W.H. Cook, A constitutive model and data for metals subjected to large strains, high strain rates and high temperatures, in: Proceedings of the 7th International Symposium on Ballistics, the Hague, the Netherlands, 19-21 April 1983.
[9] N.J. Hoff, Q. Appl. Math. **12**, 49-55 (1954).
[10] A.S. Khan, Y.S. Suh, R. Kazmi, Int. J. Plast. **20**, 2233-2248 (2004).
[11] J. Litonski, Plastic flow of a tube under adiabatic torsion, Bull. Pol. Acad. Sci.-Te. **25**, 7-17 (1977).
[12] P.S. Follansbee, U.F. Kocks, Acta Metall. **36**, 82-93 (1988).
[13] F.J. Zerilli, R.W. Armstrong, J. Appl. Phys. **61**, 1816-1825 (1987).
[14] S. Nemat-Nasser, W.G. Guo, V.F. Nesterenko, S.S. Indrakanti, Y.-B. Gu , Mech. Mater. **33**, 425-439 (2001).
[15] A. Rusinek, J.A. Rodríguez-Martínez, J.R. Klepaczko, R.B. Pęcherski, Mater. Design **30**, 1748-1761 (2009).
[16] A. Rusinek, J.A. Rodríguez-Martínez, A. Arias, Int. J. Mech. Sci. **52**, 120-135 (2010).
[17] W. Moćko, A. Brodecki, L. Kruszka, Mech. Mater. **92**, 18-27 (2016).
[18] R. Hill, Proc. Roy. Soc. London A**193**, 281-297 (1948).
[19] W. Hosford, On the yield loci of anisotropic cubic metals, In: A Arbor (Ed.), 7th North American Metalworking Conf. Michigan, USA, 13-16 May, 1979, pp. 191-197. ASME Michigan.
[20] F. Barlat, R.C. Becker, Y. Hayashida, Y. Maeda, M. Yanagawa, K. Chung, J.C. Brem, D.J. Lege, K. Matsui, S.J. Murtha, S. Hattori, Int. J. Plast. **13**, 385-401 (1997).
[21] A.P. Karafillis, M.C. Boyce, J. Mech. Phys. Solids **41**, 1859-1886 (1993).
[22] W. Sumelka, M. Nowak, Int. J. Numer. Anal. Met. **40**, 651-675 (2016).
[23] O. Cazacu, B. Plunkett, F. Barlat, Int. J. Plasticity **22**, 1171-1194 (2006).
[24] J. Ostrowska-Maciejewska, R.B. Pęcherski, P. Szeptyński, Eng. Trans. 60, 125-138 (2012).
[25] W. Moćko, A. Brodecki, Mater. Design **88**, 320-330 (2015).
[26] H. Kolsky, Proc. Phys. Soc. **62B**, 647-700 (1949).
[27] G.H. Staab, A.A. Gilat, Exp. Mech. **31**, 232-235 (1991).
[28] W. Moćko, A. Brodecki, J. Radziejewska, J. Strain Analysis **50**, 571-58 (2015).
[29] W. Moćko, Metrol. Meas. Syst. **20**, 555-564 (2013).
[30] W.I. Lankford, S.C. Snyder, J.A. Bauscher, Transaction ASM **42**, 1196-1232 (1950).
[31] A. Rusinek, J.R. Klepaczko, Int. J. Plast. **17**, 87-115 (2001).
[32] J.R. Klepaczko, A general approach to rate sensitivity and constitutive modeling of FCC and BCC metals. In: W.J. Ammann, W.K. Liu, J.A. Studer (Eds.), Impact: Effects of Fast Transient Loadings 26-27 August 1987, pp. 3-35., Rotterdam: A.A. Balkema 1988.
[33] R. Kapoor, S. Nemat-Nasser, Metall. Mater. Trans. **31A**, 15-823 (2000).
[34] M. Huang, P. Rivera-Diaz-del-Castillo, O. Bouaz, S. van der Zwaag, Mech. Mater. **41**, 982-988 (2009).
[35] W. Sumelka, T. Łodygowski, J. Eng. Mater.-T ASME **135**, 021009 (2013).
[36] D.R. Chichili, K.T. Ramesh, K.J. Hemker, Acta Mater. **46**, 1025-1043 (1998).
[37] A.S. Khan, S. Yu, H. Liu, Int. J. Plast. **38**, 14-26 (2012).
[38] D.A.S. Macdougall, J. Harding, J. Mech. Phys. Solids **47**, 1157-1185 (1999).